Constraint energy minimizing generalized multiscale finite element method for highly heterogeneous compressible flow*

Leonardo A. Poveda[1][0000−0001−9057−0274], Shubin Fu[2][0000−0002−6250−0778], and Eric T. Chung[1][0000−0002−3096−3399]

[1] The Chinese University of Hong Kong, Shatin, New Territories Hong Kong SAR, China
lpoveda@math.cuhk.edu.hk,tschung@math.cuhk.edu.hk
[2] Eastern Institute for Advanced Study, China
shubinfu@eias.ac.cn

Abstract. This work presents a Constraint Energy Minimizing Generalized Multiscale Finite Element Method (CEM-GMsFEM) for solving a single-phase compressible flow in highly heterogeneous media. To discretize this problem, we first construct a fine-grid approximation using the Finite Element Method with a backward Euler time approximation. After time discretization, we use Newton's method to handle the nonlinearity in the resulting equations. To solve the linear system efficiently, we shall use the framework of CEM-GMsFEM by constructing multiscale basis functions on a suitable coarse-grid approximation. These basis functions are given by solving a class of local energy minimization problems over the eigenspaces that contain local information on heterogeneity. In addition, oversampling techniques provide exponential decay outside the corresponding local oversampling regions. Finally, we will provide two numerical experiments on a 3D case to show the performance of the proposed approach.

Keywords: Constraint energy minimization · multiscale finite element methods · compressible flow · highly heterogeneous.

1 Introduction

The phenomenon of fluid flow through heterogeneous porous materials has been studied in fields as diverse as reservoir simulation, water storage, and groundwater contamination. These problems can be prohibitively expensive to solve when applying traditional fine-scale direct techniques, primarily due to the strong heterogeneity of the geological data. Historically, the scientific community has been motivated to develop model reduction techniques. The first is the upscaling method [1], where the upscaled geological properties, such as permeability

* Eric Chung's research is partially supported by the Hong Kong RGC General Research Fund (Project number: 14304021).

ICCS Camera Ready Version 2023
To cite this paper please use the final published version:
DOI: 10.1007/978-3-031-36030-5_22

fields, are obtained by applying specific rules and then solving the problem with a mostly reduced model. The second is the multiscale method [8, 5, 10]; in this case, the solution of the problem is approximated by local basis functions, which are solutions of a class of local problems on the coarse mesh.

Among these multiscale methods, MsFEM and, in particular, its extension GMsFEM have achieved enormous success and are used in a wide range of practical applications [9, 7]. In GMsFEM, the main idea is to use appropriately designed local spectral problems to construct the multiscale basis in GMsFEM, where multiple basis functions are allowed. Therefore, the accuracy of the multiscale solution can be tuned and controlled. In a previous work [6], significant results were obtained in the context of GMsFEM. The use of other types of multiscale methods for compressible flow, for instance, [9].

In this paper, we adopt the basic idea given in [3], which is a variation of GMsFEM based on a constraint energy minimization (CEM), for single-phase nonlinear compressible flow. This method provides a better convergence rate proportional to the size of the coarse grid. Furthermore, the CEM-GMsFEM uses the concepts of oversampling and localization [10] to compute multiscale basis functions in oversampled subregions. These basis functions are given by solving a class of local energy minimization problems over the eigenspaces that contain local information on heterogeneity.

The outline of the article is organized as follows: in Section 2, we briefly introduce the formulation of the model used in this work. Section 3 is devoted to constructing the offline multiscale space and framework of CEM-GMsFEM. Numerical experiments are presented in Section 4. Conclusions and final comments are given in Section 5.

2 Formulation of the problem

We consider the following single-phase nonlinear compressible flow through a porous medium:

$$\begin{aligned} \partial_t(\phi\rho) - \nabla\cdot\left(\tfrac{\kappa}{\mu}\rho\nabla p\right) &= q, \quad \text{in } \Omega_T := \Omega\times(0,T],\\ \tfrac{\kappa}{\mu}\rho\nabla p\cdot n &= 0, \quad \text{on } \Gamma_N\times(0,T],\\ p &= p^D, \quad \text{on } \Gamma_D\times(0,T],\\ p &= p_0, \quad \text{on } \Omega\times\{t=0\}. \end{aligned} \tag{1}$$

Here, ϕ is the porosity of the medium, which is assumed to be a constant in our presentation, p is the fluid pressure we aim to seek, and μ is the constant fluid viscosity. κ denotes the permeability field that may be highly heterogeneous. Ω is the computational domain with boundary defined by $\partial\Omega_T = \Gamma_D\cup\Gamma_N$, and n is the outward unit-normal vector on $\partial\Omega_T$. The fluid density ρ is a function of the fluid pressure p as

$$\rho(p) = \rho_{\text{ref}}e^{c(p-p_{\text{ref}})}, \tag{2}$$

where ρ_{ref} is the given reference density and p_{ref} is the reference pressure.

ICCS Camera Ready Version 2023
To cite this paper please use the final published version:
DOI: 10.1007/978-3-031-36030-5_22

Throughout this paper, we adopt the notation $L^2(D)$ and $H^1(D)$ to indicate the usual Sobolev spaces on subdomain $D \subset \Omega$ equipped with the norm $\|\cdot\|_{0,D}$ and $\|\cdot\|_{1,D}$ respectively. If $D = \Omega$, we omit the subscript D. In addition, we denote $\mathrm{V} := \mathrm{H}^1(D)$, $\mathrm{V}_0 := \mathrm{H}_0^1(D)$.

In the CEM-GMsFEM considered in this work, multiscale basis functions will be constructed for the pressure p. First, we introduce the notion of the two-scale grid. Then, we divide the computational domain Ω into some regular coarse blocks and denote the resulting triangulation as $\mathcal{T}^H$. We use H to represent the diameter of the coarse block $K \in \mathcal{T}^H$. Each coarse block will be further divided into a connected union of conforming fine-grid blocks across coarse-grid edges. We denote this fine-grid partition as $\mathcal{T}^h$, a refinement of $\mathcal{T}^H$ by definition. Let N^c be the number of coarse nodes, $\{x_i\}_{i=1}^{N^c}$ the set of nodes in $\mathcal{T}^H$ and $\omega_i = \bigcup\{K_j \in \mathcal{T}^H : x_i \in \overline{K}_j\}$ the neighborhood of the node x_i. In addition, given a coarse block K_i, we represent the oversampling region $K_{i,m} \subset \Omega$ obtained by enlarging K_i with m coarse grid layers, see Fig. 1. Let V_h be the space of the

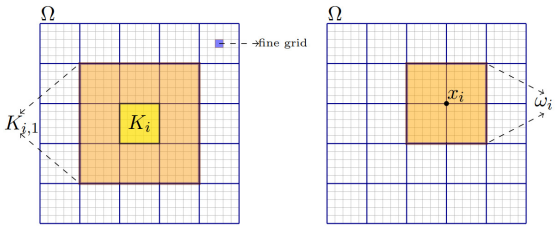

Fig. 1. Illustration of the coarse element K_i and oversampling domain $K_{i,1}$, the fine grid element and neighborhood ω_i of the node x_i.

first-order Lagrange basis function concerning the fine-grid $\mathcal{T}^h$. Then, the finite element approximation to (1) on the fine grid is to seek

$$(\phi\partial_t\rho(p_h), v) + \left(\tfrac{\kappa}{\mu}\rho(p_h)\nabla p_h, \nabla v\right) = (q, v), \quad \text{for each } v \in \mathrm{V}_h. \tag{3}$$

To derive the fully discrete scheme for (3), we introduce a partition of the time interval $[0, T]$ into subintervals $[t^{n-1}, t^n]$, $1 \le n \le N_t$ (N_t is an integer) and we denote the time-step size by $\Delta_t^n = t^n - t^{n-1}$. Then, using the backward Euler scheme in time, we can obtain the fully discrete scheme as follows: find p_h^n such that

$$(\phi\rho(p_h^n), v) - (\phi\rho(p_h^{n-1}), v) + \Delta_t^n \left(\tfrac{\kappa}{\mu}\rho(p_h^n)\nabla p_h^n, \nabla v\right) = \Delta_t^n (q, v), \tag{4}$$

for each $v \in \mathrm{V}_h$. Newton's method can solve the nonlinear equation (4). Specifically, let $\{\eta_i\}_{i=1}^{N^f}$ be the finite element basis functions for V_h, where N^f is the number of fine grid nodes. We now can write $p_h^{n,k} = \sum_i p_i^{n,k}\eta_i$ and $p_h^{n-1} = \sum_i p_i^{n-1}\eta_i$, k denotes the k-th Newton iteration. Then, we can recast the non-

ICCS Camera Ready Version 2023
To cite this paper please use the final published version:
DOI: 10.1007/978-3-031-36030-5_22

linear equation (4) as a residual equation system:

$$\begin{aligned} F_j^{n,k} =&\Big(\phi\rho\Big(\textstyle\sum_{i=1}^{N^f} p_i^{n,k}\eta_i\Big),\eta_j\Big)-\Big(\phi\rho\Big(\textstyle\sum_{i=1}^{N^f} p_i^{n-1}\eta_i\Big),\eta_j\Big) \\ &+\Delta_t^n\Big(\tfrac{\kappa}{\mu}\rho\Big(\textstyle\sum_{i=1}^{N^f} p_i^{n,k}\eta_i\Big)\textstyle\sum_{i=1}^{N^f} p_i^{n,k}\nabla\eta_i,\nabla\eta_j\Big)-\Delta_t^n(q,\eta_j)=0, \end{aligned} \tag{5}$$

for $j = 1, 2, \cdots, N^f$. To linearize the global problem, we should compute the partial derivatives of the residual equation concerning the unknown $p_i^{n,k}$, thus

$$\begin{aligned} J_{ji}^{n,k} := \frac{\phi\partial F_j^{n,k}}{\partial p_i^{n,k}} =&(\phi\rho(p_h^{n,k})\eta_i,\eta_j)+\Delta_t^n\big(\tfrac{\kappa}{\mu}\rho(p_h^{n,k})\nabla\eta_i,\nabla\eta_j\big) \\ &+\Delta_t^n\big(c\tfrac{\kappa}{\mu}\eta_i\rho(p_h^{n,k})\textstyle\sum_i p_i^{n,k}\nabla\eta_i,\nabla\eta_j\big), \end{aligned} \tag{6}$$

which results in a linear system that needs to solve $\mathbf{J}^{n,k}\boldsymbol{\delta}_{p^{n,k}} = -\mathbf{F}^{n,k}$, where $\mathbf{J}^{n,k} := [J_{ji}^{n,k}]_{i,j=1}^{N^f}$ represents the Jacobi matrix, $\mathbf{F}^{n,k} := [F_j^{n,k}]_{j=1}^{N^f}$ is the residual and $p^{n,k+1} = p^{n,k} + \boldsymbol{\delta}_{p^{n,k}}$.

3 Construction of multiscale basis function

This section is devoted to the framework of CEM-GMsFEM and introduces the construction of multiscale spaces. We emphasize that the multiscale basis functions and corresponding spaces are defined concerning the coarse grid $\mathcal{T}^H$. The multiscale method consists of two stages. In the first stage, we construct the auxiliary multiscale basis function using the framework of the generalized multiscale finite element method (GMsFEM) [5]. In the second stage, we construct the multiscale basis function by solving some energy-minimizing problem in the coarse oversampling region $K_{i,m}$ with $m \geq 1$, see [3].

We construct auxiliary multiscale basis functions by solving the spectral problem for each coarse element K_i. We make use of the space V restricted to the coarse element K_i, *i.e.*, $\mathrm{V}(K_i) := \mathrm{V}\big|_{K_i}$. Then, we solve the following local eigenvalue problems: find $(\lambda_j^{(i)}, \varphi_j^{(i)}) \in \mathbb{R} \times \mathrm{V}(K_i)$ such that

$$a_i(\varphi_j^{(i)}, w) = \lambda_j^{(i)} s_i(\varphi_j^{(i)}, w), \quad \text{for each } w \in \mathrm{V}(K_i), \tag{7}$$

where $a_i(v, w) := \int_{K_i} \kappa\rho(p_0)\nabla v \cdot \nabla w dx$, and $s_i(v, w) := \int_{K_i} \widetilde{\kappa} v w dx$, in which $\widetilde{\kappa} = \rho(p_0)\kappa \sum_{i=1}^{N^c} |\nabla\chi_i|^2$, N^c is the total number of neighborhoods, p_0 is the initial pressure p and $\{\chi_i\}$ are the partitions of unity function of ω_i [2].

We assume that the eigenfunctions satisfy the normalized condition $s_i(\varphi_j^{(i)}, \varphi_j^{(i)}) = 1$. The eigenvalues are ordered ascendingly, *i.e.*, $\lambda_1^{(i)} \leq \lambda_2^{(i)} \leq \cdots$. Then, we can use the first L_i eigenfunctions to construct the local auxiliary multiscale $\mathrm{V}_{\mathrm{aux}}(K_i) := \mathrm{span}\{\varphi_j^{(i)} : 1 \leq j \leq L_i\}$. Then, the global auxiliary space $\mathrm{V}_{\mathrm{aux}}$ is defined by using these local auxiliary spaces $\mathrm{V}_{\mathrm{aux}} = \bigoplus_{i=1}^{N^c} \mathrm{V}_{\mathrm{aux}}(K_i)$.

The inner product and s-norm of the global auxiliary multiscale spaces are defined respectively by $s(v, w) = \sum_{i=1}^{N^c} s_i(v, w)$, $\|v\|_s := \sqrt{s(v, v)}$.

ICCS Camera Ready Version 2023
To cite this paper please use the final published version:
DOI: 10.1007/978-3-031-36030-5_22

To construct the CEM-GMsFEM basis functions, we use the following definition from [3].

Definition 1 ($\varphi_j^{(i)}$**-orthogonality).** *Given a function* $\varphi_j^{(i)} \in \mathrm{V}_{\mathrm{aux}}$*, if a function* $\psi \in \mathrm{V}$ *satisfies*

$$s(\psi, \varphi_j^{(i)}) = 1, \quad s(\psi, \varphi_{j'}^{(i')}) = 0, \quad \text{if } j' \neq j \text{ or } i' \neq i,$$

then, we say that is $\varphi_j^{(i)}$*-orthogonal where* $s(v, w) = \sum_{i=1}^{N} s_i(v, w)$.

We define the operator $\pi : \mathrm{V} \to \mathrm{V}_{\mathrm{aux}}$ by $\pi(v) = \sum_{i=1}^{N} \sum_{j=1}^{L_i} s_i(v, \varphi_j^{(i)})\varphi_j^{(i)}$, for each $v \in \mathrm{V}$, and the null space of the operator π is defined by $\widetilde{\mathrm{V}} = \{v \in \mathrm{V} : \pi(v) = 0\}$.

We will now construct the multiscale basis functions. For each coarse block K_i, we define the oversampled subdomain $K_{i,m} \subset \Omega$ by enlarging K_i with an arbitrary number of coarse grid layers $m \geq 1$. Let $\mathrm{V}_0(K_{i,m}) := \mathrm{H}_0^1(K_{i,m})$; we solve the following minimization problems: find multiscale basis function $\psi_{j,\mathrm{ms}}^{(i)} \in \mathrm{V}_0(K_{i,m})$

$$\psi_{j,\mathrm{ms}}^{(i)} = \mathrm{argmin}\{a(\psi, \psi) : \psi \in \mathrm{V}_0(K_{i,m}),\ \psi \text{ is } \varphi_j^{(i)}\text{-orthogonal}\}. \tag{8}$$

Then, the CEM-GMsFEM space is defined by

$$\mathrm{V}_{\mathrm{ms}} = \mathrm{span}\{\psi_{j,\mathrm{ms}}^{(i)} : 1 \leq j \leq L_i, 1 \leq i \leq N\}.$$

The minimization problem (8) is implicit; we can redefine it into an explicit form by using a Lagrange multiplier. Then, the problem (8) can be written as the following problem: find $\psi_{j,\mathrm{ms}}^{(i)} \in \mathrm{V}_0(K_{i,m})$, $\lambda \in \mathrm{V}_{\mathrm{aux}}^{(i)}(K_i)$ such that

$$\begin{cases} a(\psi_{j,\mathrm{ms}}^{(i)}, \eta) + s(\eta, \lambda) & = 0, \quad \text{for all } \eta \in \mathrm{V}(K_{i,m}), \\ s(\psi_{j,\mathrm{ms}}^{(i)} - \varphi_j^{(i)}, \nu) & = 0, \quad \text{for all } \nu \in \mathrm{V}_{\mathrm{aux}}^{(i)}(K_{i,m}), \end{cases}$$

where $\mathrm{V}_{\mathrm{aux}}^{(i)}(K_{i,m})$ is the union of all local auxiliary spaces for $K_i \subset K_{i,m}$. Note that one can solve the above continuous problem numerically on a fine-scale grid. Thus, given the above space and by using the backward Euler scheme, the full-discrete formulation reads as follows: find $p_{\mathrm{ms}} \in \mathrm{V}_{\mathrm{ms}}$ such that

$$(\phi\rho(p_{\mathrm{ms}}^n), v) - (\phi\rho(p_{\mathrm{ms}}^{n-1}), v) + \Delta_t^n \left(\tfrac{\kappa}{\mu}\rho(p_{\mathrm{ms}}^n)\nabla p_{\mathrm{ms}}^n, \nabla v\right) = \Delta_t^n(q, v), \tag{9}$$

for all $v \in \mathrm{V}_{\mathrm{ms}}$. The local multiscale basis construction is motivated by the global basis construction defined below.

4 Numerical results

In this section, we present two representative examples to confirm the performance of the CEM-GMsFEM. We use the backward Euler scheme for the time

ICCS Camera Ready Version 2023
To cite this paper please use the final published version:
DOI: 10.1007/978-3-031-36030-5_22

discretization and Newton's method for the nonlinear equation. All computations are performed by using the software `MatLab`. Firstly, we consider two high-contrast permeability fields for each experiment. Long channels and inclusions form these fields, the blank regions have values of 10^5 millidarcys, while other regions have values of 10^9 millidarcys (see, for instance, Fig. 2). In all numerical tests, we let viscosity $\mu = 5$cP, porosity $\phi = 500$, fluid compressibility $c = 1.0 \times 10^{-8}1/\text{Pa}$, the reference pressure $p_{\text{ref}} = 2.00 \times 10^7\text{Pa}$, and the reference density $\rho_{\text{ref}} = 850\text{kg}/\text{m}^3$.

We consider the first experiment a full zero Neumann boundary condition, with an initial pressure field p_0 with value $2.16 \times 10^7\text{Pa}$. Four vertical injectors are placed in the corners, and one sink is in the middle of the domain to drive the flow. We set the fine grid resolution of 64^3, with fine grid size of $h = 20\text{m}$, the coarse grid resolution of 8^3, with $H = 8h$. The parameter Δ_t^n is 7 days, and $T = 20\Delta_t^n (= 140$ days) is the total simulation time. For the CEM-GMsFEM, we use 4 basis function and 4 oversampling layers. It is clear that the number of bases efficiently improves the accuracy of the CEM-GMsFEM [3]; in this case, the relative L^2 error is 1.7396E-03 and H^1 error is 3.8180E-01. The dimension of the coarse system is 4916 ($= 729 \times$ number of basis functions); note that the dimension of the fine-scale system is 274625. We compare the pressure profiles with singular source and zero Neumann boundary conditions in Fig. 2.

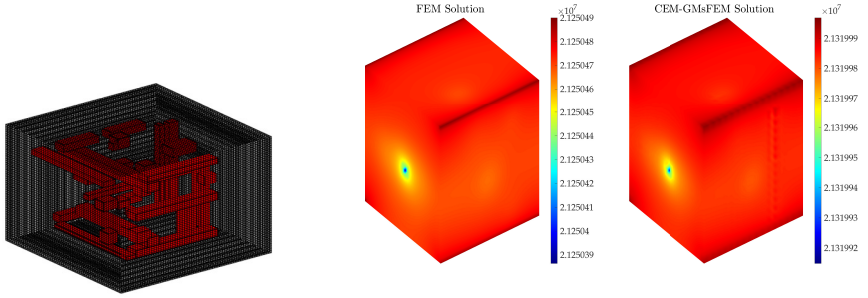

Fig. 2. Experiment with full-zero Neumann boundary condition. High-contrast permeability field (left), fine-scale reference solution (middle), and CEM-GMsFEM solution (right) with 4 basis function and 4 oversampling layers at $T = 20\Delta_t^n$.

In the second experiment, we consider a zero Neumann boundary condition and nonzero Dirichlet boundary condition [11]. We impose zero Neumann condition on boundaries of planes xy and xz and let $p = 2.16 \times 10^7\text{Pa}$ in the first yz plane and $p = 2.00 \times 10^7\text{Pa}$ in the last yz plane for all time instants, no additional source is imposed. The pressure difference will drive the flow, and the initial field p_0 linearly decreases along the x axis and is fixed in the yz plane. Table 1 shows that numerical results use 4 basis functions on each coarse block with different coarse grid sizes ($H = 4h, 8h$ and $16h$). In Table 1, ε_0 and ε_1

ICCS Camera Ready Version 2023
To cite this paper please use the final published version:
DOI: 10.1007/978-3-031-36030-5_22

denote the relative L^2 and energy error estimate between the reference solution and CEM-GMsFEM solution.

In Fig. 3, we depict the numerical solution profiles with a fine grid resolution of 32^3 and coarse grid resolution of 8^3 at $T = 140$ day, which have a good agreement. For this case, by using 4 basis functions and the coarse grid size $H = 8h$, the CEM-GMsFEM uses 4 oversampling layers, and the relative error $\varepsilon_0 = 2.8514\text{E-}04$, while $\varepsilon_1 = 3.8213\text{E-}01$.

Table 1. Numerical result with different numbers of oversampling layers (m) for the second experiment with full zero Neumann and nonzero Dirichlet boundary condition.

Number basis	H	Number oversampling layers m	ε_0	ε_1
4	$4h$	3	2.3493E-03	5.6700E-01
4	$8h$	4	2.8514E-04	3.8213E-01
4	$16h$	5	1.3302E-04	1.6102E-01

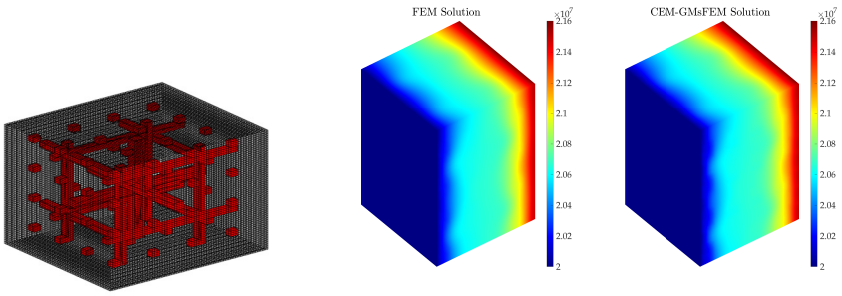

Fig. 3. Experiment with combined boundary condition. High-contrast permeability field (left), fine-scale reference solution (middle), and CEM-GMsFEM solution (right) with 4 basis function and 4 number of oversampling layers at $T = 20\Delta_t^n$.

5 Conclusions and future directions

We have presented CEM-GMsFEM for solving the highly heterogeneous nonlinear single-phase compressible flow in this work. For CEM-GMsFEM, the first step is constructing the additional space by solving spectral problems. The second step is based on constraint energy minimization and oversampling. So, we construct multiscale basis functions for pressure. Two representative 3D examples have been presented to verify the efficiency and accuracy of the proposed method. The convergence depends on the coarse mesh size and the decay of eigenvalues of local spectral problems. In addition, the CEM-GMsFEM is shown

ICCS Camera Ready Version 2023
To cite this paper please use the final published version:
DOI: 10.1007/978-3-031-36030-5_22

to have a second-order convergence rate in the L^2-norm and a first-order convergence rate in the energy norm concerning the coarse grid size.

In some applications, a future challenge remains to boost the performance of the coarse-grid simulation, especially when the source term is singular; one may need to further improve the accuracy of the approximation without additional mesh refinement. In these cases, one needs to enrich the multiscale space by adding more basis functions in the online stage [4]. These new basis functions are based on the oversampling technique and the information on local residuals. Moreover, an adaptive enrichment algorithm will be presented to reduce error in some regions with large residuals.

References

1. Arbogast, T., Xiao, H.: A multiscale mortar mixed space based on homogenization for heterogeneous elliptic problems. SIAM J. Numer. Anal. **51**(1), 377–399 (2013)
2. Babuška, I., Melenk, J.M.: The partition of unity method. Internat. J. Numer. Methods Engrg. **40**(4), 727–758 (1997)
3. Chung, E.T., Efendiev, Y., Leung, W.T.: Constraint energy minimizing generalized multiscale finite element method. Comput. Methods Appl. Mech. Engrg. **339**, 298–319 (2018)
4. Chung, E.T., Efendiev, Y., Leung, W.T.: Fast online generalized multiscale finite element method using constraint energy minimization. J. Comput. Phys. **355**, 450–463 (2018)
5. Efendiev, Y., Galvis, J., Hou, T.Y.: Generalized multiscale finite element methods (GMsFEM). J. Comput. Phys. **251**, 116–135 (2013)
6. Fu, S., Chung, E., Zhao, L.: Generalized Multiscale Finite Element Method for Highly Heterogeneous Compressible Flow. Multiscale Model. Simul. **20**(4), 1437–1467 (2022)
7. Fu, S., Chung, E.T.: A local-global multiscale mortar mixed finite element method for multiphase transport in heterogeneous media. J. Comput. Phys. **399**, 108906, 13 (2019)
8. Hou, T.Y., Wu, X.H.: A multiscale finite element method for elliptic problems in composite materials and porous media. J. Comput. Phys. **134**(1), 169–189 (1997)
9. Kim, M.Y., Park, E.J., Thomas, S.G., Wheeler, M.F.: A multiscale mortar mixed finite element method for slightly compressible flows in porous media. J. Korean Math. Soc. **44**(5), 1103–1119 (2007)
10. Må lqvist, A., Peterseim, D.: Localization of elliptic multiscale problems. Math. Comp. **83**(290), 2583–2603 (2014)
11. Wang, Y., Hajibeygi, H., Tchelepi, H.A.: Algebraic multiscale solver for flow in heterogeneous porous media. Journal of Computational Physics **259**, 284–303 (2014)

ICCS Camera Ready Version 2023
To cite this paper please use the final published version:
DOI: 10.1007/978-3-031-36030-5_22